

Monte Carlo tuning in the presence of Matching

B. Cooper¹, J. Katzy², M. L. Mangano³, A. Messina³, L. Mijović², P. Skands³

¹ Department of Physics & Astronomy, University College London, WC1E 6BT, UK

² Deutsches Electron Synchrotron, 22603 Hamburg, Germany

³ European Organization for Nuclear Research, CERN CH-1211, Geneva 23, Switzerland

Abstract

We consider the impact of varying α_s choices (and scales) on each side of the so-called “matching scale” in MLM-matched matrix-element + parton-shower predictions of collider observables. We explain how inconsistent prescriptions can lead to counter-intuitive results and present a few explicit examples, focusing mostly on W/Z + jets processes. We give a specific prescription for how to improve the consistency of the matching and also address how to perform consistent tune variations (e.g., of the renormalization scale) around a central choice. Comparisons to several collider processes are included to illustrate the properties of the resulting improved matching, relying on AlpGen + Pythia 6, with the latter using the so-called Perugia 2011 tunes, developed as part of this effort.

1 Introduction

The theoretical description of multijet production in hadronic collisions is one of the key ingredients for the interpretation of the data from high-energy hadron colliders, the 1.96 TeV proton-antiproton Tevatron collider at Fermilab, and the proton-proton Large Hadron Collider (LHC) at CERN. Final states with multijets, possibly associated with electroweak gauge bosons, are in fact the dominant signature of the decay of heavy particles produced at high energy, whether in the Standard Model (top quarks and Higgs bosons), or in theories beyond the Standard Model (BSM), such as supersymmetry. The identification of these particles, and the study of their properties, requires an accurate modelling of the Standard Model (SM) sources of multijets. Great progress was achieved towards this goal in the past decade. On one side, the calculation of inclusive, parton-level, cross-sections to next-to-leading-order (NLO) in QCD has produced results for processes as complex as $W+4$ jets [1]. On the other, algorithms have been developed and implemented in numerical codes to provide a complete description of the hadronic final states emerging from processes with up to 6 jets, merging the exact leading-order (LO) calculation of the partonic matrix elements (ME) with the evolution, provided by so-called shower Monte Carlo (MC) codes, of the partonic shower (PS) and the subsequent hadronization of the partons in to physical hadrons.

The development of theoretical tools has been accompanied by experimental measurements, which provide the necessary validation test-bed for these calculations. Parton-level NLO calculations provide a first-principle description of inclusive final states: they have an intrinsic high degree of precision, due to the reduced dependence on the unphysical choice of a renormalization and factorization scale and, furthermore, are not subject to modelling uncertainties related to the details of the non-perturbative phase of the final state evolution. Calculations based on the merging of LO matrix elements, shower evolution and hadronization, on the other hand, while affected by the larger scale-setting uncertainty due to the LO approximation, provide a fully exclusive description of the final states, and are therefore more suitable for the experimental analyses. Their ultimate goal is not only to give reliable estimates of the inclusive jet rates and energy distributions, but also to reproduce properties of the final states such as the jet inner structure and the distribution of softer particles produced outside of the jets, including those resulting from the evolution of the fragments of the original colliding hadrons¹. These properties, which depend on the details of the non-perturbative dynamics, can only be described through the phenomenological models embedded in the shower MC codes. The parameters of these phenomenological models need to be tuned using experimental data of some suitable observables. The factorization assumption built into any description of large- Q processes justifies the use of these same parameters in the prediction of different observables, and provides the basis for the predictive power of such tools. This assumption however must be validated with a direct comparison with data. Elements that need to be probed include the scaling with beam energy of the UE parameters, the universality of the parameters controlling the shower evolution and hadronization, and the overall independence of all parameters on the type of hard process. Deviations from the expected universality would highlight faults in the underlying modelling of effects beyond perturbative physics, or could be due to the insufficient precision of the perturbative description, in case NLO effects were to modify significantly the LO predictions. Differences compatible with the theoretical systematics of the LO approximation could however be reabsorbed by modifying the perturbative parameters that govern the LO systematics, for example the renormalization and factorization scales, or the matching variables used in the matrix-element/shower merging algorithm.

It is therefore important to understand the correlations between the effects of changing the soft and UE parameters on one side, and the perturbative parameters on the other. In this paper we present studies which

¹We refer to the ensemble of these particles as the underlying event, or UE

demonstrate that, in the tuning of ME-PS matched predictions, it is vital that there is consistency in the treatment of α_S in both the ME and PS components. While this is a general issue for all shower MCs, we consider as an explicit example the merging of LO matrix elements with the Pythia 6 shower MC [2], as implemented in the framework of the AlpGen code [3], one of the reference tools for experimental multijet studies at the Tevatron and at the LHC. The most recent versions of Pythia (6.425) and AlpGen (2.14) codes were used for producing the results.

On the Pythia 6 side, we consider several different tune variations of the interleaved p_T -ordered parton-shower model [4], focusing on the so-called “Perugia” set of tunes of [5, 6], ranging from the Perugia 0 tune (from 2009) to the Perugia 2011 updates that have been developed as part of this work, including systematic up/down variations of the shower activity (see the Appendix and [5, 6] for details). We also compare to the “DW” tune [7] of the virtuality-ordered shower model [8, 9]. For Herwig [10], we include the “Jimmy” underlying-event model [11], with default parameters. We emphasize that the qualitative conclusions presented in this paper carry over to other shower models, including the ones implemented in Pythia 8 [12, 13] and Herwig ++ [14], but the quantitative aspects should still be considered limited to the particular tunes and shower models studied here. We rely on Fastjet [15] for jet clustering and have further used the Rivet-based [16] mcplots web site [17] for some of our comparisons.

The paper is organised as follows: in Section 2 we describe in detail the theoretical nature of the α_S consistency problem, and give a practical example of how it can be manifest in the prediction of high p_T observables. In Section 3 we show how a simple prescription can be applied to stabilise ME-PS tunings against this problem, propose a new tune for AlpGen + Pythia 6 matched predictions, and demonstrate the behaviour of this tune under tuning variations. In Section 4 we show that this new AlpGen + Pythia 6 tune is able to reproduce (within statistical errors) the Tevatron and LHC vector boson plus jets data. In addition we also the tune predictions to the jet shape measurements at the Tevatron and LHC. Finally we conclude in Section 5.

2 The Importance of Consistent α_S Treatment in ME-PS Matched Predictions

In this section we demonstrate that consistent treatment of α_S in ME-PS matched predictions is important in order to achieve the desired accuracy in the prediction of high p_T observables. We first present the theoretical arguments behind this, and then go on to show and explain that without adopting this approach one can observe undesirable and counter-intuitive effects on experimental observables.

2.1 Theoretical Background

The philosophy behind matching prescriptions such as the MLM one [18, 19] employed by AlpGen is to separate phase space cleanly into two distinct regions; a short-distance one, which is supposed to be described by matrix elements, and a long-distance one described by parton showers. In the long-distance region, real and virtual corrections, with the latter represented by Sudakov factors, are both generated by the shower and are intimately related by unitarity (for pedagogical reviews, see, e.g., [20, 21]). On the short-distance side, the real corrections are generated by the matrix elements while the virtual ones are still generated by the shower.

Much effort has gone into ensuring that the behaviour across the boundary between the two regions be as smooth as possible. CKKW showed [22] that it is possible to remove any dependence on this “matching scale” at NLL precision by careful choices of all ingredients in the matching; technical details of the implementation are important, and the dependence on the unphysical matching scale may be larger than NLL unless the implementation matches the theoretical algorithm precisely [23–25].

Especially when two different computer codes are used for matrix elements and showering, respectively (as when AlpGen or MadGraph [26] is combined with Pythia 6 or Herwig), inconsistent parameter sets between the two codes can jeopardise the consistency of the calculation and lead to unexpected results, as will be illustrated in the following sections.

To give a very simple theoretical example, suppose a matched matrix-element generator (MG) uses a different definition of α_s than the parton-shower generator (SG). Suppressing parton luminosity factors to avoid clutter, the real corrections, integrated over the hard part of phase space, for some arbitrary final state F , will then have the form

$$\sigma_{F+1}^{\text{incl}} = \int_{Q_F^2}^s d\Phi_{F+1} \alpha_s^{\text{MG}} |M_{F+1}|^2, \quad (1)$$

where we have factored out the coupling corresponding to the “+1” parton and suppressed the dependence on any other couplings that may be present in $|M_{F+1}|^2$. The virtual corrections at the same order, generated by the shower off F , will have the form

$$\sigma_F^{\text{excl}} = \sigma_F^{\text{incl}} - \int d\Phi_F \int_{Q_F^2}^s \frac{dQ^2}{Q^2} dz \sum_i \frac{\alpha_s^{\text{SG}}}{2\pi} P_i(z) |M_F|^2 + \mathcal{O}(\alpha_s^2), \quad (2)$$

with $P_i(z)$ the DGLAP splitting kernels (or equivalent radiation functions in dipole or antenna shower approaches). If the two codes use the same definitions for the strong coupling, $\alpha_s^{\text{SG}} = \alpha_s^{\text{MG}}$, then the fact that $P(z)/Q^2$ captures the leading singularities of $|M_{F+1}|^2$ guarantees that the difference between the two expressions can at most be a non-singular term. Integrated over phase space, such a term merely leads to a finite $\mathcal{O}(\alpha_s)$ change to the total cross section, which is within the expected precision. Indeed, it is a central ingredient in both the MLM and (L)-CKKW matching prescriptions that a reweighting of the matched matrix elements be performed in order to ensure that the scales appearing in α_s match smoothly between the hard and soft regions. Thus, we may assume that the choice of renormalization scale after matching is $\mu \sim p_T$ on both sides of the matching scale, where p_T is a scale characterising the momentum transfer at each emission vertex, as established by [27, 28] and encoded in the CKKW formalism [22].

In the case of the CKKW approach as implemented in the Sherpa MC framework [29], this prescription can be controlled exactly, since the matrix element and the shower evolution are part of the same computer code and hence naturally use the same α_s definition. This is also true in Lönnblad’s variant [23] of the algorithm, used in Ariadne [30]. In the case of codes like AlpGen or Madgraph, on the other hand, an issue emerges. These codes are designed to generate parton-level event samples to be used with an arbitrary shower MC. Different shower MCs however use slightly different scales for the parton branchings, as a result of different approaches to the shower evolution, and may use different values of Λ_{QCD} , as a result of the tuning of the showers and/or underlying events. A possible mismatch therefore arises in the values of α_s used by the matrix-element calculation and those used by the shower.

If there is a mismatch in Λ_{QCD} or $\alpha_s(M_Z)$, then this will effectively generate a real-virtual difference whose leading singularities are proportional to

$$\alpha_s^2 b_0 \ln \left(\frac{\Lambda_{\text{MG}}^2}{\Lambda_{\text{SG}}^2} \right) \frac{dQ^2}{Q^2} \sum_i P_i(z) |M_F|^2. \quad (3)$$

	A	B	C
Λ_{MG}	Λ	$\frac{1}{2}\Lambda$	Λ
Λ_{SG}	Λ	Λ	$\frac{1}{2}\Lambda$

Table 1: The three cases, A, B, and C discussed in the text, for an arbitrary reference Λ value.

which is of next-to-leading logarithmic order (unless $\Lambda_{\text{MG}} \sim \Lambda_{\text{SG}}$, in which case it vanishes). Similarly, even if both matrix-element and shower codes are using the same Λ_{QCD} , but they use different running orders, then there will be an $\mathcal{O}(\alpha_s^3 \ln(p_T^2/\Lambda^2))$ mismatch, which may also become large if $p_T \gg \Lambda$.

To be more concrete, let us consider a specific example. Compare A) a matched MG+SG calculation which uses the same Λ_{QCD} value on both sides of the matching to B) a calculation in which the value used on the MG side is reduced to half its previous value but the SG one remains the same, as summarised by the two first columns of tab. 1. Going from case A to B, the following changes result:

1. The number of $(F + 1)$ states added by the MG decreases, due to the lowering of the Λ_{QCD} value on the MG side, while the number of surviving F states remains constant, since the shower Sudakov is not modified. The total estimated cross section therefore decreases.
2. At the differential level, the smaller number of $(F + 1)$ states combined with the unchanging number of F states implies smaller absolute jet cross sections and smaller fractions $\sigma_{\text{jet}}/\sigma_{\text{tot}}$.

Similarly we may consider what happens if C) we reduce the Λ_{QCD} value on the SG side instead, as summarised in the last column of tab. 1. Going from case A to C, the following changes result:

1. The number of $(F + 1)$ states added by the MG remains constant, while the number of surviving F states increases, since the SG is generating fewer branchings. The total estimated cross section therefore *increases*.
2. Since the number of $(F + 1)$ states is constant, while the shower is made less active, the final jets will actually be narrower, which *increases* the rate of reconstructed jets at any given fixed p_T value.
3. Since both the total cross section increases and the number of reconstructed additional jets also increases, jet *fractions* can either increase or decrease.

In particular, note the somewhat counter-intuitive effect that *decreasing* the shower α_s value actually *increases* the jet rates in a matched calculation, while it normally *decreases* them in a standalone shower calculation.

Since, as was discussed above, inconsistencies among the choices on the two sides can lead to differences at the NLL level, it is obviously important to ensure that they are consistent within a reasonable margin. This is particularly true in the context of event-generator tuning, in which specifically the NLL components of the shower description are sought to be optimized with respect to measured data, and hence changes at this level could effectively destroy the tuning.

Finally, we remind the reader that a change in Λ_{QCD} can be interpreted as a change in the opposite direction of the renormalization scale argument (for constant Λ_{QCD}), modulo small flavour threshold effects that we

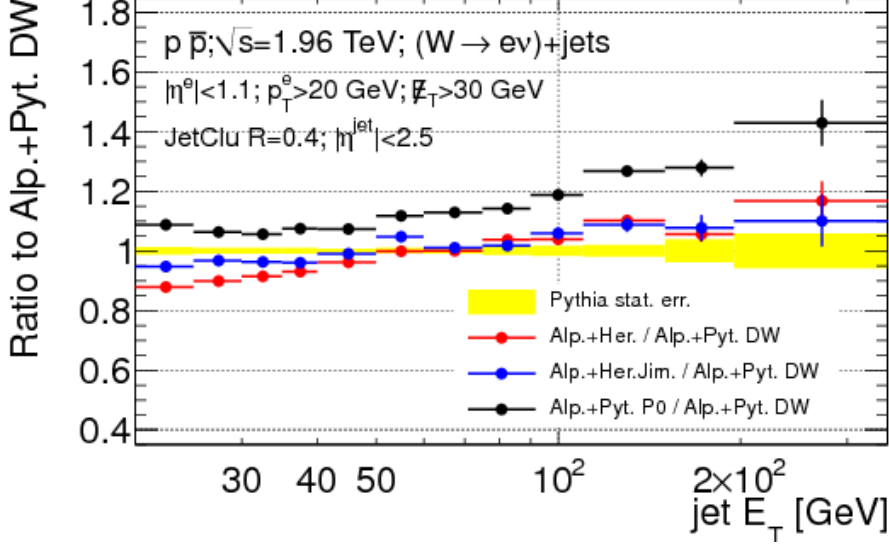


Figure 1: Ratio of predictions for the leading-jet E_T spectrum in W+jets final states at the Tevatron, obtained with AlpGen plus various MC codes and tunes. The leading jet observable is defined at the particle-level as in the CDF W+jets analysis [32].

shall ignore here. This is easy to realise from the definition of the coupling,

$$\alpha_s(k\mu^2) \stackrel{1\text{-loop}}{=} \frac{1}{b_0 \ln(k\mu^2/\Lambda^2)} = \frac{1}{b_0 \ln(\mu^2/(\frac{1}{k}\Lambda^2))} . \quad (4)$$

Thus, we may write renormalization scale variations (e.g., by a factor of 2 in each direction) either by applying a prefactor directly on the renormalization scale argument of α_s or by applying the inverse of that factor to Λ_{QCD} while keeping the renormalization scale argument unchanged. Due to the technical structure of the codes, the former is more convenient in AlpGen (via the `ktfac` setting) whilst the latter is more convenient for Pythia 6.

2.2 Examples of the interplay between tunes and matching

In this section we give several examples of how the issues in ME-PS matching described in Section 2 can affect high- p_T observables using AlpGen interfaced to Pythia 6 with DW [7], Perugia 0 (P0) [5, 31] and Perugia 2010 (P2010) tunes [6].

In Fig. 1 we show the ratio of predictions for the transverse energy (E_T) spectrum of the leading jet (that jet with the highest E_T per event) in W+jet final states at the Tevatron, obtained by the merging of AlpGen with different shower codes; Herwig, Pythia 6 virtuality-ordered shower (DW), and p_T -ordered shower (Perugia 0). The differences between Herwig and Herwig plus Jimmy at small E_T can be explained by the different amounts of energy that, in the various cases, are deposited by the UE in the jet cones. In particular, as shown in Fig. 2, these differences can accommodate the slight shape discrepancy between data and AlpGen +Herwig that was noted, at small E_T , in the CDF study [32]. It is difficult, however, to attribute to the UE energy the significant differences seen in Fig. 1 at large E_T .

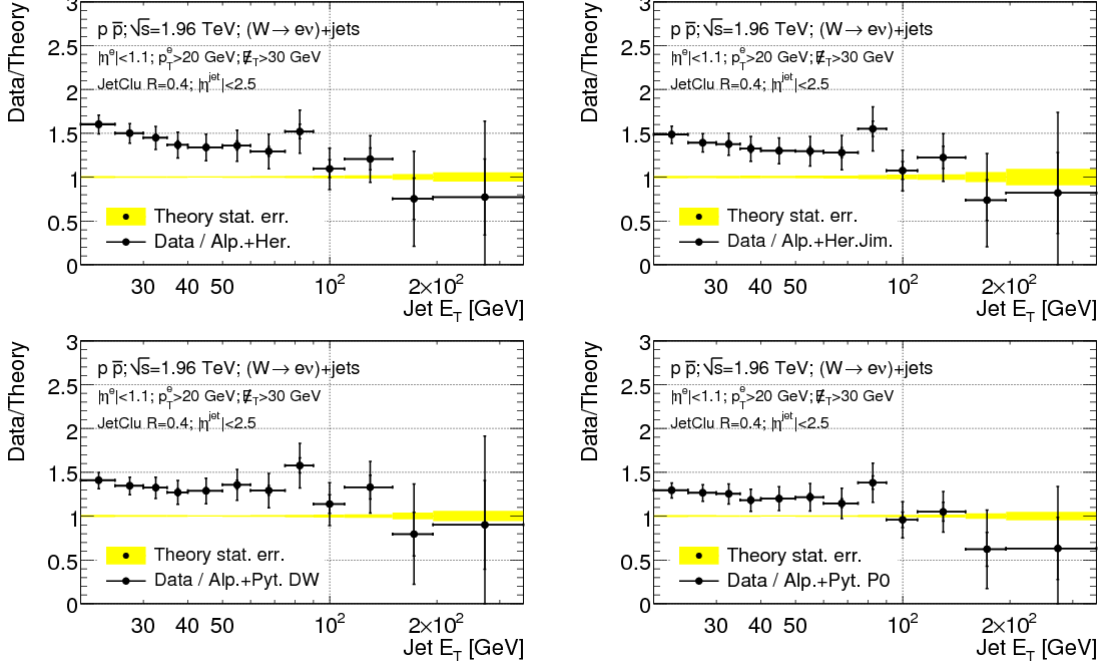


Figure 2: Comparison of CDF data [32] with the leading-jet E_T spectrum predicted by AlpGen plus various MC codes and tunes.

In order to investigate the source of the differences in the predictions, systematic parameter variations of the perturbative and non-perturbative model components of Pythia 6 have been studied using the Perugia family of Pythia 6 tunes with Perugia 0 as the central tune and Perugia Hard and Perugia Soft as the systematic variation tunes. The Perugia Soft and Perugia Hard tunes both use the same Parton Density Function (PDF) as Perugia 0, CTEQ5L [33], but differ in the values of Pythia 6 parameters controlling both perturbative and non-perturbative activity levels. In comparison to Perugia Soft, the Perugia Hard tune has more perturbative (initial and final state radiation) activity but less non-perturbative (multiple interactions, beam remnant and hadronization) activity. Perugia Soft on the other hand has less perturbative but more non-perturbative activity than the Perugia 0 tune. In order to investigate the interplay of the tuning variations with the MLM matching, the effect of the change of the tune on the physics observables in both the Pythia 6 standalone case and AlpGen + Pythia 6 case is presented.

In Fig. 3 the distribution of jet multiplicity (N_{jet}) in W +jets events is compared for events generated with the Perugia 0, Perugia Hard and Perugia Soft tunes. The N_{jet} observable is defined at the particle-level according to the definition used in the ATLAS measurement of the W +jets cross-section at $\sqrt{s}=7$ TeV [34]. Jets are clustered from stable particles using the anti-Kt jet algorithm [35] with the radius parameter $R = 0.4$, and considered in case they satisfy the following kinematic cuts: $p_T > 20$ GeV and $|\eta| < 2.8$. Comparisons are performed for both the Pythia 6 standalone (left) and AlpGen + Pythia 6 (right) cases. For the Pythia 6 standalone case we observe that Perugia Hard tune yields more high- p_T jets than the Perugia 0 tune while Perugia Soft yields less final state jets correspondingly. For the AlpGen + Pythia 6 case an opposite trend is observed: Perugia Hard tune yields less high- p_T jets and Perugia Soft tune yields more high- p_T jets. In order to determine which modelling components of the Perugia Soft and Perugia Hard tunes cause this behaviour, we considered the effect of varying individual sets of parameters of the Perugia Soft and Perugia Hard tunes

in AlpGen + Pythia 6 predictions. Parameters were grouped according to the modelling aspect they control into Initial State Radiation (ISR), Final State Radiation including the FSR from the ISR partons (FISR), the Underlying Event (UE) and Colour Reconnections (CR) blocks²

Dedicated samples where only parameters of an individual block were varied in the ranges used in Perugia Soft and Perugia Hard tunes on top of the Perugia 0 tune were produced. The results of the study, in terms of the cross-section contribution of each AlpGen sub-sample (after MLM matching), are given in Table 2. As was already noted in Fig. 3, the cross-section for multijet production in the Perugia Hard case decreases with respect to Perugia 0, and vice versa for Perugia Soft. From Table 2, we see that the parameter blocks that produce this affect are the ISR and FISR blocks, while the impact of the CR and UE block variations on the cross-sections is negligible. In addition to the simultaneous variations of parameters in the blocks, we have also performed individual parameter variations for each of the parameters in order to check that potential correlations between the parameters do not affect the conclusions. Studies have also been performed for the Hadronization and Beam Remnant blocks of [6]. The variations of these parameters also had a negligible effect on the kinematic distributions and cross-section values.

In Fig. 4 we demonstrate that the increased parton shower activity can indeed lead to the reduced cross-section (and softer jet spectra) due to the increased rates at which the AlpGen + Pythia 6 events are vetoed during the MLM matching. In the figure the distributions of the events that pass or fail (ISVETO=0 or ISVETO≠0) the MLM matching criterion are shown for the exclusive sub-sample of AlpGen + Pythia 6 Perugia 2010 W+jets events with exactly three additional partons from the matrix element in the final state³. Each of the distributions is normalised to unit area. The distributions are shown as a function of the largest p_T shower emission from the initial state radiation (left) and as a function of the largest p_T multiple proton-proton interaction.⁴ In the left hand side figure we see that the events are rejected with higher probability, the larger the p_T of the hardest ISR branching in the event. Therefore, a Pythia 6 standalone tune which increases the ISR activity can, somewhat counter-intuitively, reduce the rate for multijet and hard emissions. In the right hand side we demonstrate that the events are accepted and rejected independently of the transverse momentum of the hardest multiple interaction in the event (which is the desired behaviour of the matching application used with the parton shower code).

To conclude, the origin of the differences observed in the predictions of tunes with different ISR/FSR activity matched to AlpGen is rather due to the mismatch between the jet-emission probability predicted by the matrix elements and by the shower. This comes from the mismatch in the value of α_s discussed earlier, arising from different values of Λ_{QCD} or from the use of a different evolution variable in the shower. If the value of α_s in the shower increases, the emission rate of additional jets during the shower evolution will increase. Since the matching algorithm rejects events with extra jets generated by the shower, to replace them with events where the jet is accounted for by a higher-order matrix element calculation, a larger value of α_s in the shower leads to a higher rejection rate. Unless this change in α_s is accompanied by a similar change in the matrix element calculation, the additional rejection is not compensated by the relative increase in rate for the higher-order parton-level contributions, leading to the effects reported in this section.

This important interplay between MC parameters, which are typically tuned to “soft” observables such as UE or the small- p_T DY spectrum, and the performance of the matching algorithms for “hard” observables, calls for particular attention when adopting new UE tunes in the framework of multijet studies with matrix-element matching. Along the same lines, it should be kept in mind that, tuning a stand-alone shower MC to

²The parameter blocks organisation is similar to the one introduced in [6] and are listed in A.2

³The observations in the text are largely independent on the final state parton multiplicity

⁴These p_T values are reported by Pythia 6 parameters VINT(357) (ISR) and VINT(359) (MPI) respectively.

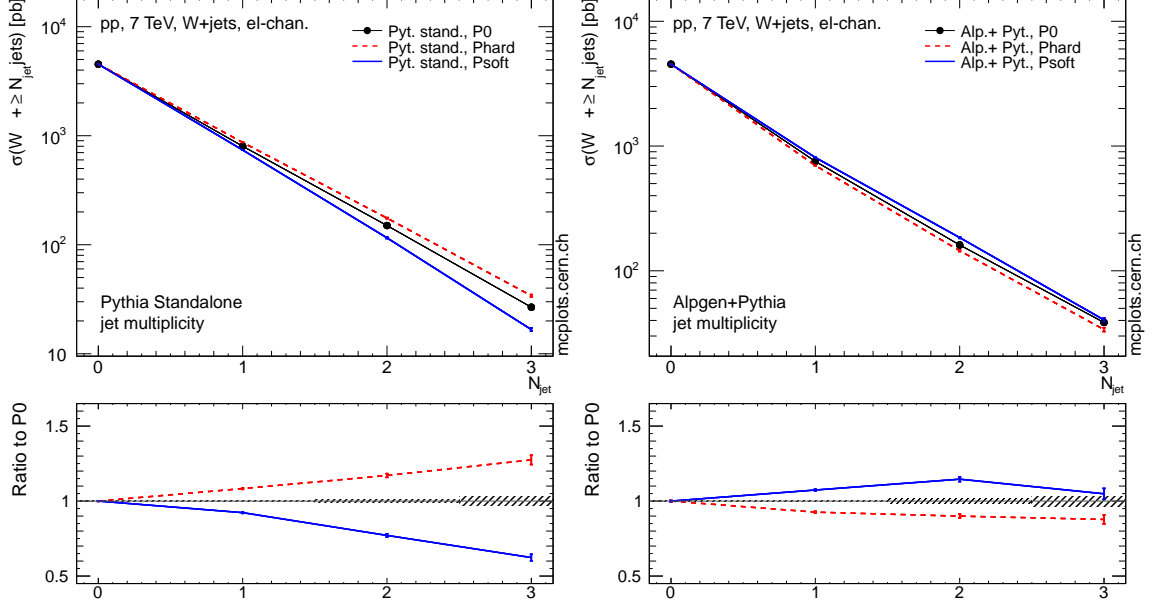


Figure 3: Jet ($p_T > 20$ GeV and $|\eta| < 2.8$) multiplicity distribution in W +jets electron channel events in pp collisions at 7 TeV. Distributions are shown for the samples generated with Pythia 6 standalone (left) and with Alpgen + Pythia 6 (right). For each case the distributions obtained when using Perugia 0 (P0), Perugia Hard (Phard) and Perugia Soft (Psoft) tunes are shown. All distributions are scaled so that the value of the first bin agrees with the ATLAS measurement [34].

tune	Np0	Np1	Np2	Np3	Np4+	total [pb]
Phard	7287 ± 3.9	728 ± 2.6	141 ± 1.3	27 ± 0.2	6.6 ± 0.2	8190 ± 8
P0	7556 ± 3.6	814 ± 2.7	166 ± 1.3	32 ± 0.3	7.8 ± 0.3	8576 ± 8
Psoft	7804 ± 3.4	944 ± 2.8	207 ± 1.5	42 ± 0.3	10.1 ± 0.3	9007 ± 8
P0 with Phard ISR	7207 ± 6.9	735 ± 2.6	143 ± 1.3	27 ± 0.2	6.9 ± 0.2	8119 ± 11
P0 with Psoft ISR	7831 ± 4.9	881 ± 2.7	186 ± 1.4	36 ± 0.3	8.8 ± 0.3	8943 ± 10
P0 with Phard FISR	7548 ± 6.0	814 ± 2.7	167 ± 1.3	32 ± 0.3	7.8 ± 0.3	8569 ± 10
P0 with Psoft FISR	7505 ± 6.1	878 ± 2.7	188 ± 1.4	37 ± 0.3	9.4 ± 0.3	8617 ± 10
P0 with Phard UE	7513 ± 6.1	826 ± 2.7	171 ± 1.4	33 ± 0.3	7.8 ± 0.3	8551 ± 10
P0 with Psoft UE	7576 ± 5.9	817 ± 2.7	166 ± 1.3	32 ± 0.3	8.1 ± 0.3	8599 ± 10
P0 with Phard CR	7561 ± 5.9	821 ± 2.7	167 ± 1.3	32 ± 0.3	8.1 ± 0.3	8589 ± 10
P0 with Psoft CR	7556 ± 5.9	815 ± 2.7	165 ± 1.3	32 ± 0.3	8.1 ± 0.3	8576 ± 10

Table 2: Impact of different variations of the Pythia 6 Perugia 2010 tunes on the cross sections of Alpgen W +jets sub-samples with different matrix element parton multiplicities, and the total inclusive W cross section. For the studies sub-samples with up to four additional partons from the matrix element were generated. The matching is performed inclusively for the highest parton multiplicity sub-sample and exclusively for other sub-samples. The tabulated cross-sections were extracted after the MLM matching and parton shower. The errors shown are statistical only. The parameter settings of the various setups are discussed in the text.

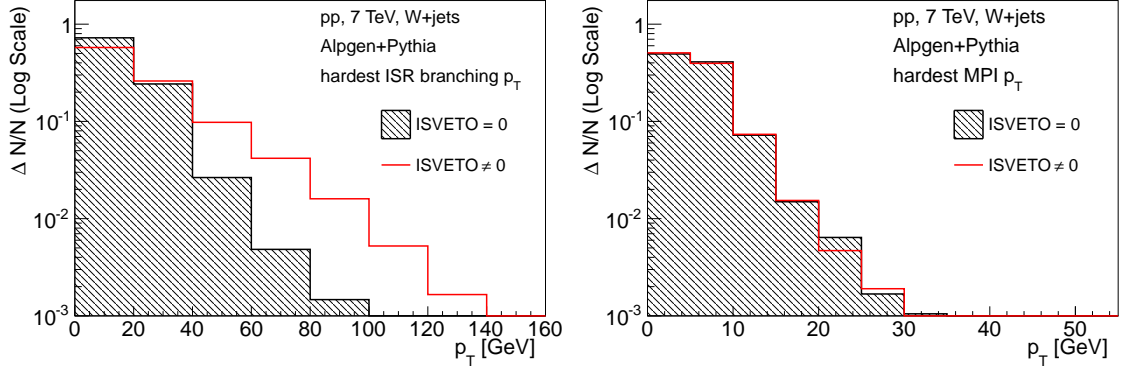


Figure 4: Distribution of the probabilities for the event acceptance (ISVETO=0) or rejection (ISVETO \neq 0) during the MLM matching step, as a function of the largest p_T shower emission from the initial state radiation (left) and the largest p_T multiple proton-proton interaction in the event (right). The events were generated using exclusive sub-sample of AlpGen + Pythia 6 Perugia 2010 W+jets events with exactly three additional partons from the matrix element in the final state for pp collisions at 7 TeV and AlpGen + Pythia 6 Perugia 2010 tune.

better model multijet final states, will force it to emulate effects present in the multiparton matrix elements. Using such tunes with matrix-element matching therefore requires ad-hoc modifications of the matching algorithm, or of its parameters.

3 Stabilising ME-PS Matched Tunings

In this section we discuss how to overcome the problems discussed in the previous section with a simple prescription, and outline a tuning strategy that should allow to consistently optimize, in the context of the Pythia 6 shower MC, the description of both the UE and the high- E_T properties of final states.

3.1 A New AlpGen + Pythia 6 α_S Consistent Tune

As it was explained in Section 2.1, and practically demonstrated in Section 2.2, it is highly desirable to have a consistent treatment of α_S on either side of the ME and PS boundary. In Appendix A.1 the relevant settings for a new α_S consistent AlpGen + Pythia 6 tune are described in detail. In this tune, the α_S consistency is essentially ensured by setting the effective value of Λ_{QCD} to be the same throughout the Pythia 6 parton shower algorithms and in the AlpGen matrix elements. A consistent choice for Λ_{QCD} of

$$\Lambda_{\text{QCD}}^{(5)} \sim 0.26, \quad (5)$$

is made, where the superscript indicates the number of flavours. This choice is informed by comprehensive Professor tunings [36, 37] of the p_T -ordered shower in Pythia 6 [4] to event shapes and other LEP data. Note that the settings for Pythia 6 are those of the central Perugia 2011 (P2011) tune [6], which was inspired by these studies. We will refer to this new tune of AlpGen + Pythia 6 as the Perugia 2011 “matched” tune.

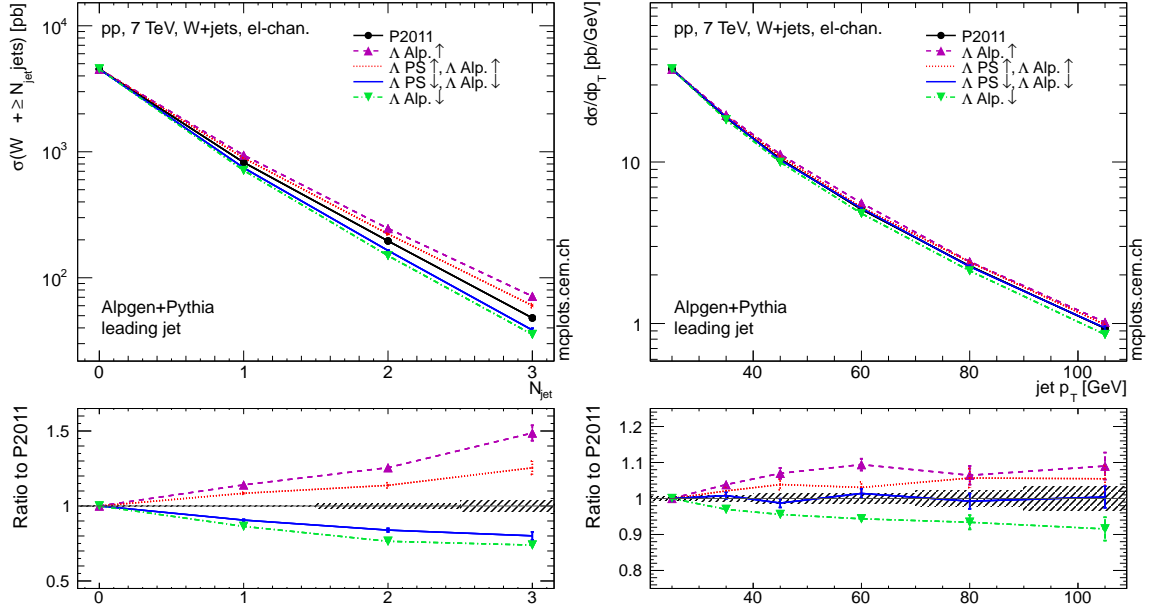


Figure 5: Comparison of AlpGen + Pythia 6 ($p_T > 20$ GeV) jet multiplicity (left) and leading jet transverse momentum (right) distributions in W +jets electron channel events. The samples are generated using different AlpGen + Pythia 6 parameter setups described in the text.

3.2 Tests of the Consistent α_s Approach: Behaviour Under Scale Variations

In this section we study the behaviour of the new AlpGen + Pythia 6 Perugia 2011 “matched” tune under Λ_{QCD} variations to demonstrate that, with a consistent treatment of α_s , the expected behaviour of ME-PS matched predictions under variations of tuning parameters is restored. W +jets events selected with the same criteria applied for Fig. 3 are used. Figure 5 shows the jet multiplicity (left) and leading jet transverse momentum (right) distributions for the Perugia 2011 “matched” tune and four variant tune samples generated with different Λ_{QCD} values. Two samples, labelled as “ Λ Alp. \uparrow ” and “ Λ Alp. \downarrow ”, have Λ_{QCD} respectively increased and decreased by a factor of 2 only in the ME calculation. This is achieved by setting respectively the AlpGen parameter $ktfac$ to 1/2 and 2. The increase (decrease) of the Λ_{QCD} value in AlpGen results in more (less) jets and a harder (softer) leading jet spectrum as shown in Fig. 5. The two samples labelled as “ Λ PS \uparrow , Λ Alp. \uparrow ” and “ Λ PS \downarrow , Λ Alp. \downarrow ” correspond to a consistent variation of Λ_{QCD} both in the ME and PS, with Λ_{QCD} respectively increased and decreased by a factor of 2. The impact of these variations is qualitatively similar to the case where Λ_{QCD} is only varied in the ME, restoring the expected behaviour of ME-PS matched prediction under variation of Λ_{QCD} . However, the samples with Λ_{QCD} varied simultaneously in the ME and in the PS exhibit a smaller deviation from the nominal sample. The mitigation of the impact of a Λ_{QCD} coherent change in a ME-PS matched sample compared to the same change only in the ME calculation is due to the interplay between the radiation produced by PS and the matching algorithm, as detailed in Section 2.1. While the choice of the $x1clu$ parameter allows to directly adapt AlpGen to possible future changes in the choice of Λ_{QCD} in Pythia, the variation of the $ktfac$ parameter in the standard range $0.5 < ktfac < 2$ can be used to establish the range of the systematical uncertainty, or to tune the description of specific observables.

4 Comparisons with Data

In this section we demonstrate that the new Λ_{QCD} -consistent Perugia 2011 “matched” tuning of AlpGen + Pythia 6 introduced in Section 3.1 compares well with recent Tevatron and LHC measurements, and that, with the arrival of improved precision measurements, there should be room for further tuning of these predictions.

4.1 Z/W+jets production

The figures that follow show comparisons of AlpGen + Pythia 6 Monte Carlo predictions to measurements of published Z+jets and W+jets processes from CDF [32, 38, 39] and W+jets from ATLAS [40]⁵. These cross-section measurements are corrected for all known detector effects to particle level and compared to Monte Carlo predictions. The Monte Carlo predictions of V+jet production cross-sections are formed by clustering the stable final state particles ($\tau > 10$ ps) following parton shower and hadronization of the unweighted events. This clustering is done using the same jet algorithm as the measurement, as implemented in the Fastjet [15] package. All stable final state particles are used, with the exception of the leptons that result from the decay of the signal W or Z boson. The decay leptons are corrected for the final state QED radiation such that their 4-momentum is equivalent to that before radiation. After the events have been clustered, the restrictions on the allowed phase space of the jets and of the W/Z boson decay products are applied to be consistent with the measurement to which we are comparing. The prediction of the final AlpGen + Pythia 6 cross-sections contains contributions from V+0, 1, 2, 3 parton samples (showered with exclusive MLM matching), and V+4 parton samples (showered with inclusive MLM matching).

Two different AlpGen + Pythia 6 generations are compared to the data; the new AlpGen + Pythia 6 Perugia 2011 “matched” tune introduced in Section 3.1 (labelled “Alp.+Pyt. P2011”), and an AlpGen + Pythia 6 prediction using the default settings of AlpGen and the Pythia 6 DW tune (labelled “Alp.+Pyt. DW”). The ratio of the matched predictions to the data are shown and compared. Additionally, the results of variations of $k_t\text{fac}$ by factors of 0.5 and 2.0 in the AlpGen + Pythia 6 Perugia 2011 “matched” prediction are shown as solid lines. The hatched regions show the total error (statistical plus systematic) propagated to the theory/data ratio from the data measurements. The error bars on the points show the statistical error on the theoretical prediction.

In Figure 6 we show the ratio of the predicted theory cross-sections to the data for the CDF Z+jets measurement [39]. In this measurement jets are defined by the CDF midpoint algorithm [46], with $R_{\text{cone}} = 0.7$ and are required to have $p_T^{\text{jet}} > 30$ GeV and $|y^{\text{jet}}| < 2.1$. In Figure 7 we show the ratio of the predicted theory cross-sections to the data for the CDF W+jets measurement [32]. In this measurement jets are defined by the CDF JetClu algorithm [47], with $R_{\text{cone}} = 0.4$ and are required to have $p_T > 20$ GeV and $|\eta| < 2.5$. In Figure 8 we show the ratio of the predicted theory cross-sections to the data for the ATLAS W+jets measurements [40]. In this measurement jets are defined by the anti-Kt algorithm [35], with a radius parameter $R = 0.4$ and are required to have $p_T > 20$ GeV and $|\eta| < 2.8$.

The AlpGen + Pythia 6 Perugia 2011 “matched” prediction compares well with the measured cross sections both as a function of the inclusive jet multiplicity and jet p_T . In particular, the prediction correctly describes the low p_T region of the differential cross section and the jet sub-structure without presenting any significant disagreement with data at high p_T . This shows that it is possible to tune separately the long- and short-

⁵Measurements of these processes at the Tevatron have also been performed by D0 [41–43]. Preliminary, higher statistics, studies of W/Z+jets production at the LHC have been reported by ATLAS [34, 44], and CMS [45].

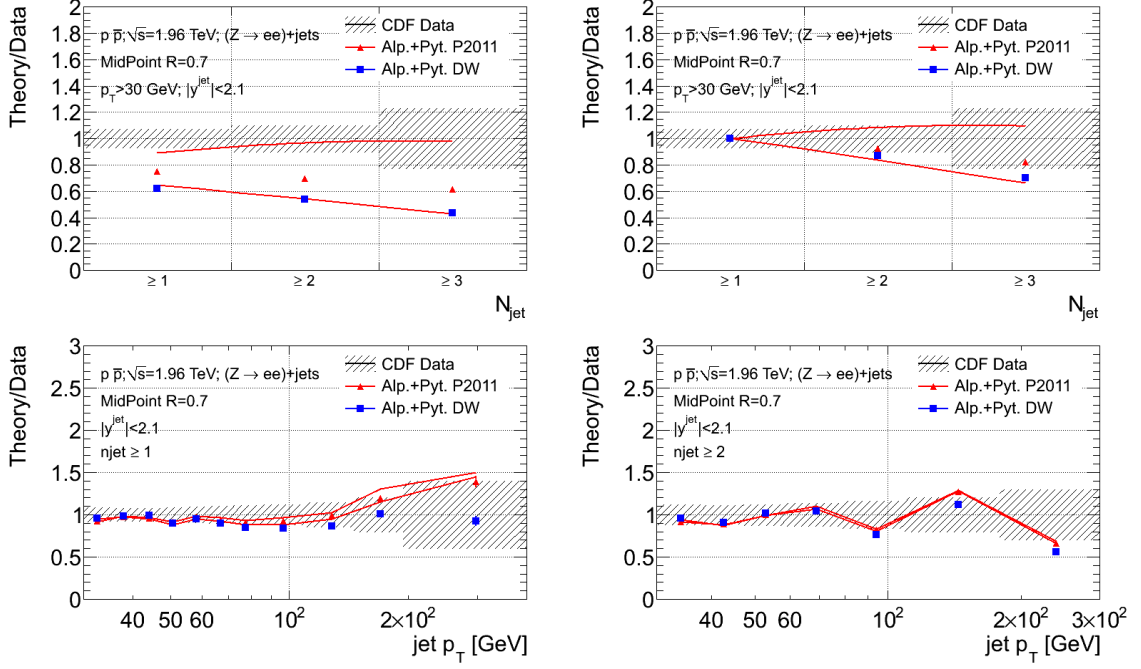


Figure 6: (Top) The ratio of predicted theory and CDF measured data cross-sections for the production of a $Z \rightarrow ee$ boson in association with at least N_{jet} jets [39]. In the left hand figure the theory predictions are not normalised to the data. In the right hand figure the theory predictions are normalised such that they equal the data measurement in the ≥ 1 jet bin. (Bottom) The ratio of predicted theory and CDF measured data cross-sections for the production of a $Z \rightarrow ee$ boson in association with at least 1 jets (left hand side) and at least 2 jets (right hand side) as a function of jet E_T . In the left hand plot, the theory prediction is normalised such that the predicted rate for ≥ 1 jet production is equal to that measured in the data. In the right hand plot, the theory prediction is normalised such that the predicted rate for ≥ 2 jet production is equal to that measured in the data.

distance contributions of the prediction to obtain a satisfactory description of the observables in the whole experimental accessible phase space. Remarkably, the prediction describes the data both at $\sqrt{s} = 1.96$ TeV and $\sqrt{s} = 7$ TeV. This illustrates that the scaling properties of the long-distance contribution with the centre of mass energy of the collision does not produce unexpected effects in the high p_T region of the cross section. A coherent rescaling of α_s with $ktfac = 0.5, 2$ has a little effect on the shapes of the differential cross-sections, while for the inclusive N_{jet} cross-sections it produces variations that bracket the default prediction. The $ktfac$ parameter can therefore be used to explore the sensitivity of the prediction to a variation of the renormalization and factorization scale, other than allow tuning on data. With the statistics of the currently available measurements there is no much room for optimising the parameters of the AlpGen + Pythia 6 Perugia 2011 “matched” prediction in a tune that better describes the measurements. However, with the imminent arrival of more precise higher-statistics LHC measurements, this should be possible in the near future.

Even though not explicitly shown here, in the relevant publications one can find similarly good agreement between the available measurements [32, 34, 44] and predictions based on AlpGen + Herwig.

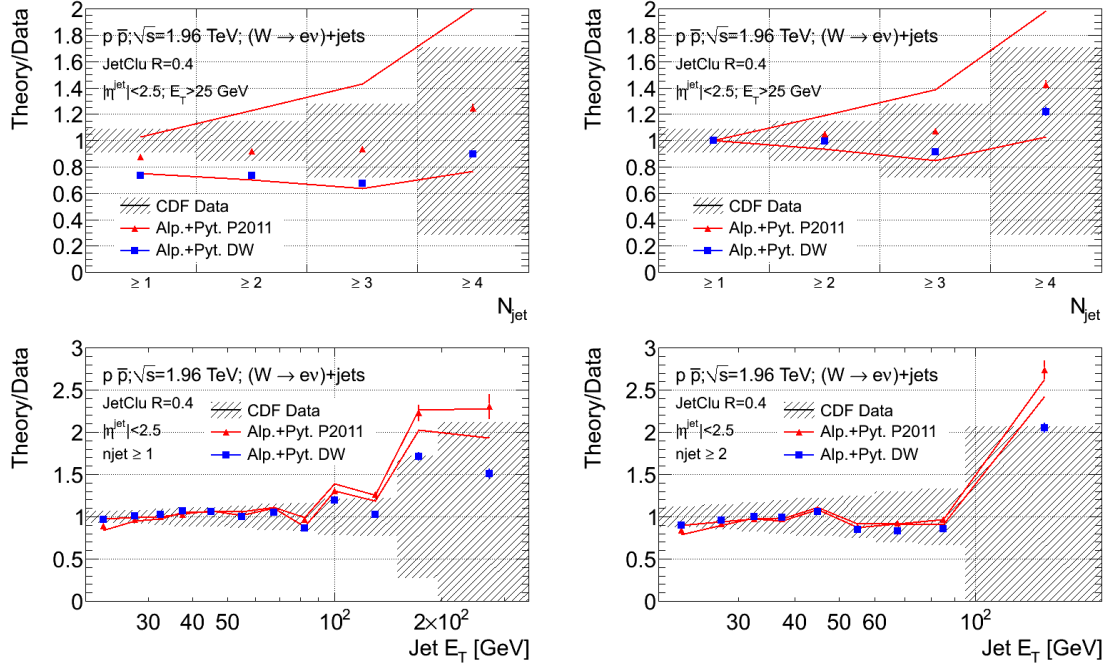


Figure 7: (Top) The ratio of predicted theory and CDF measured data cross-sections for the production of a $W \rightarrow e\nu$ boson in association with at least N_{jet} jets [32]. In the left hand figure the theory predictions are not normalised to the data. In the right hand figure the theory predictions are normalised such that they equal the data measurement in the ≥ 1 jet bin. (Bottom) The ratio of predicted theory and CDF measured data cross-sections for the production of events containing a $W \rightarrow e\nu$ boson in association with at least 1 jets (left hand side) and at least 2 jets (right hand side), as a function of the leading jet E_T (left hand side), and the sub-leading jet E_T (right hand side). In the left hand plot, the theory prediction is normalised such that the predicted rate for ≥ 1 jet production is equal to that measured in the data. In the right hand plot, the theory prediction is normalised such that the predicted rate for ≥ 2 jet production is equal to that measured in the data.

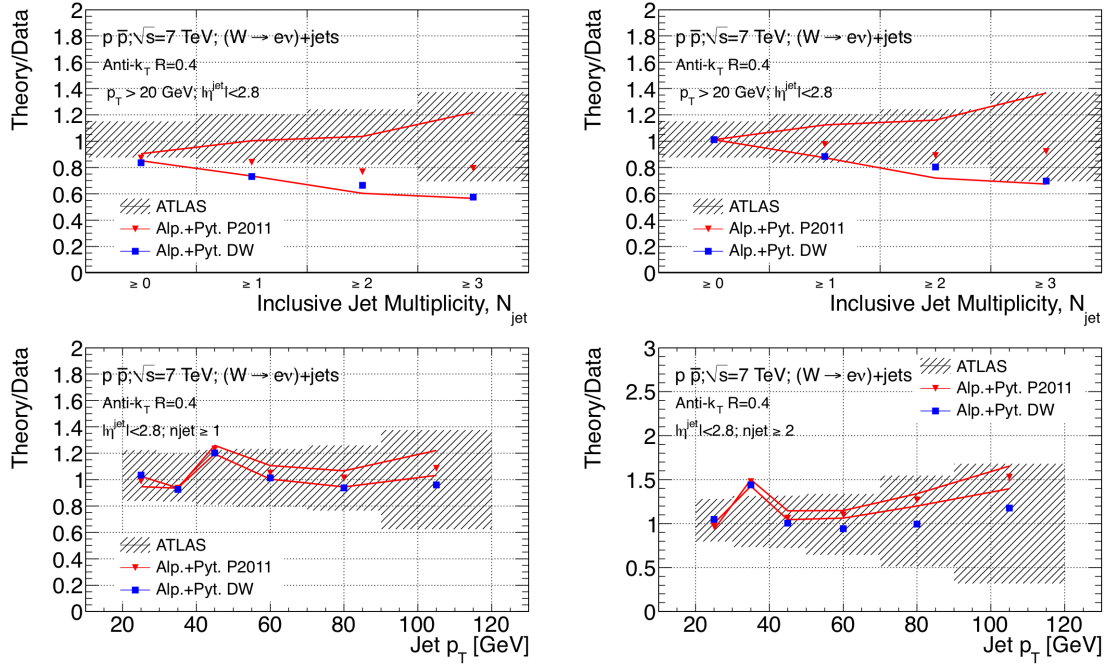


Figure 8: (Top) The ratio of predicted theory and ATLAS published cross-sections [40] for the production of a $W \rightarrow e\nu$ boson in association with at least N_{jet} jets. In the left hand figure the theory predictions are not normalised to the data. In the right hand figure the theory predictions are normalised such that they equal the data measurement in the ≥ 0 jet bin. (Bottom) The ratio of predicted theory and ATLAS data cross-sections for the production of events containing a $W \rightarrow e\nu$ boson in association with at least 1 jets (left hand side) and at least 2 jets (right hand side), as a function of the leading jet p_T (left hand side), and the sub-leading jet p_T (right hand side). In the left hand plot, the theory prediction is normalised such that the predicted rate for ≥ 1 jet production is equal to that measured in the data. In the right hand plot, the theory prediction is normalised such that the predicted rate for ≥ 2 jet production is equal to that measured in the data.

4.2 Jets shapes

Finally we test the ability of the new AlpGen + Pythia 6 Perugia 2011 “matched” tune and the systematics variations to describe the jet shapes at the LHC and the Tevatron.

For the LHC, the jet shapes measured in inclusive jet production by the ATLAS collaboration [48] are taken as reference. For this measurement the jets are reconstructed using the anti-kt algorithm with the distance parameter $R=0.6$, the transverse momentum range $30 \text{ GeV} < p_T < 600 \text{ GeV}$ and rapidity in the region $|y| < 2.8$. The jet shapes are expected to be sensitive to both perturbative (parton shower) and non-perturbative (fragmentation and underlying event) modelling aspects. We perform the data comparisons for both the AlpGen + Pythia 6 and Pythia 6 standalone cases. The samples are generated using different Pythia 6 standalone and AlpGen + Pythia 6 parameter settings as follows: for Pythia 6 standalone the Perugia 2011 and the associated systematics tunes Perugia 2011 radHi and Perugia 2011 radLo are compared. The same tunes are also used for the generating the AlpGen + Pythia 6 distributions whereby the Λ_{QCD} values are always set to the same values in AlpGen (using `ktfac`) and Pythia 6 (i.e. the Perugia 2011 “matched” central settings and the systematic variations around the central settings). The setups are compared to the integral jet shape distributions as measured in the data. The integral jet shape is defined as the average fraction of the jet p_T that lies inside a cone of radius r concentric with the jet cone [48]:

$$\Psi(r) = \frac{1}{N_{\text{jet}}} \sum_{i=1}^{N_{\text{jet}}} \frac{p_T(0, r)}{p_T(0, R)}, \quad 0 \leq r \leq R. \quad (6)$$

The sum is performed over all the N_{jet} jets in the kinematic region of interest.

In Figure 9 the integral jet shape distributions are compared to the ATLAS data for the jets in the transverse momentum ranges of 40-60 GeV (top) and 260-310 GeV (bottom) in the whole measured rapidity range ($|y| < 2.8$). We observe that both Pythia 6 standalone (left) and AlpGen + Pythia 6 (right) with Perugia 2011 provide reasonably good description of the jet shapes. Due to MLM matching the jets in the AlpGen + Pythia 6 case tend to be more narrow than in the Pythia 6 standalone case.

For the Tevatron, the shapes of jets produced in association with a Z boson as measured by CDF [49] are used. In this measurement jets are defined by the CDF midpoint algorithm [46], with $R_{\text{cone}} = 0.7$ and are required to have $p_T^{\text{jet}} > 30 \text{ GeV}$ and $|y^{\text{jet}}| < 2.1$. Figure 10 shows good agreement between AlpGen + Pythia 6 and the measurement for both the DW and Perugia 2011 tunes.

The comparisons in Figures 9 and 10 (as well as comparisons to the jet shapes in other kinematic regions and comparisons to further LHC measurements) reveal no major short-comings of the AlpGen + Pythia 6 Perugia 2011 “matched” tune. The Perugia 2011 tune has been developed by tuning Pythia 6 standalone, whereby the effective value of Λ_{QCD} was set to be the same throughout the Pythia 6 parton shower in the anticipation of using it with the AlpGen matrix elements using the same effective Λ_{QCD} value. The agreement with the measured jet shapes data could therefore potentially be improved by performing a dedicated tuning of AlpGen + Pythia 6.

5 Conclusions

We have shown that, in the context of tuning ME-PS matched predictions, it is vital that the tuning adopted ensures a consistent treatment of α_S on either side of the “matching boundary”. In the case of Alp-

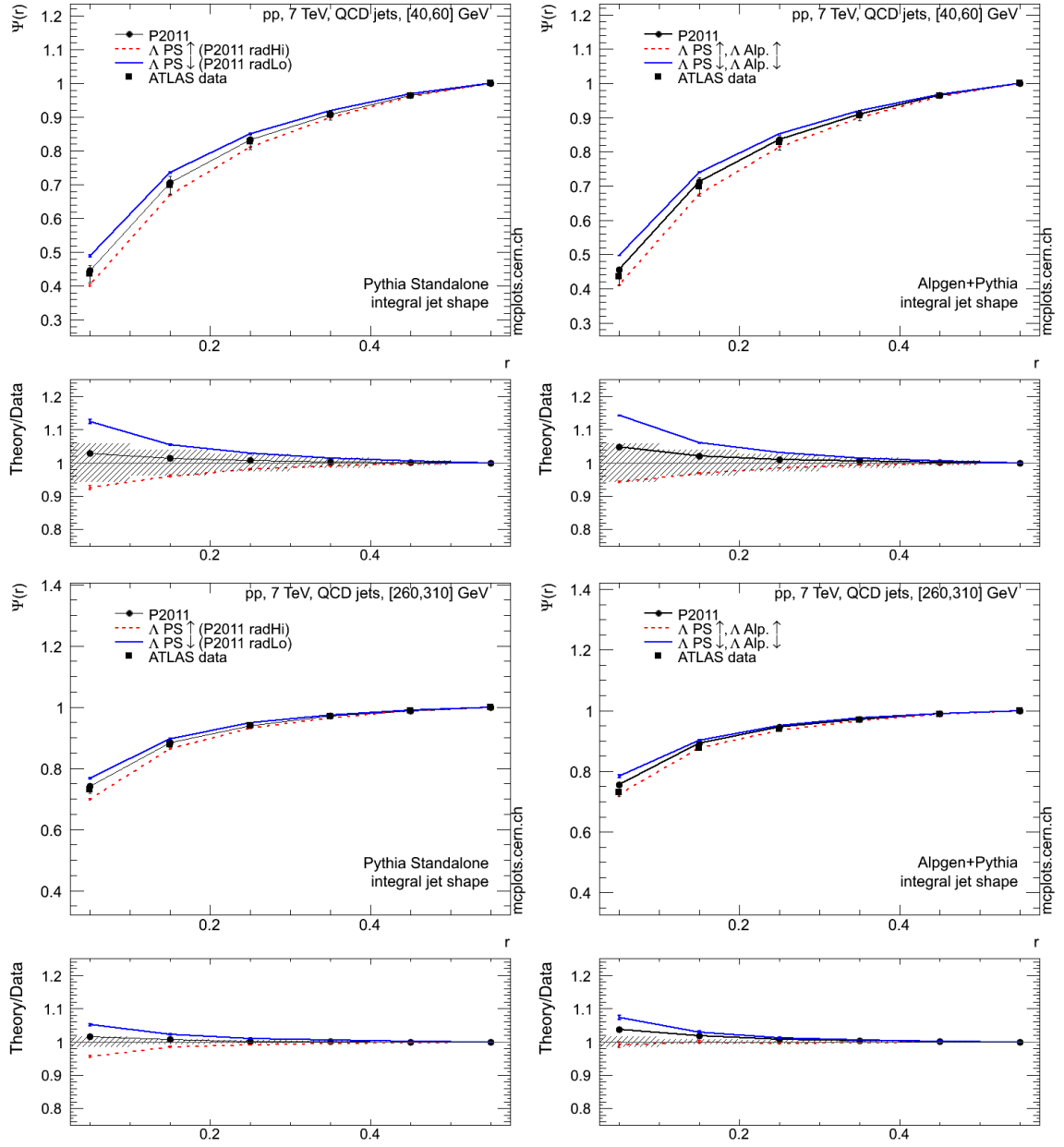


Figure 9: Comparison of the integral jet shapes as measured by ATLAS [48] with the predictions of the Pythia 6 standalone (left) and Alpgen + Pythia 6 (right) using Perugia 2011, Perugia 2011 radHi and Perugia 2011 radLo tunes. The comparisons are performed for the jets with $|y| < 2.8$ and p_T ranges of 40-60 GeV (top) and 260-310 GeV (bottom).

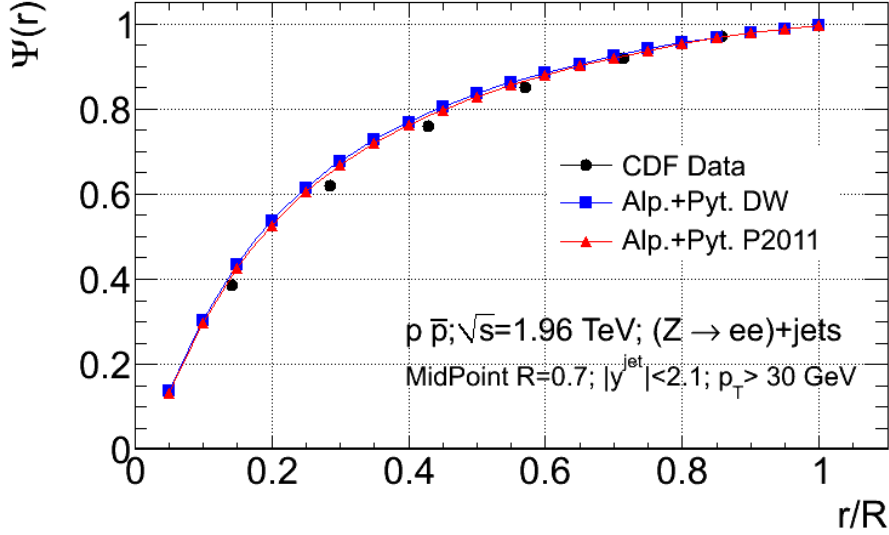


Figure 10: A comparison of the predicted and CDF measured jet shape in Z +jets events, showing the fraction of the total energy of a jet of radius R contained within a radius r , $\Psi(r)$, as a function of r/R . “Alp.+Pyt. DW” uses the default AlpGen parameters and the DW Pythia tune, “Alp.+Pyt. P2011” is described in Section 3.1 and it includes a consistent choice of Λ_{QCD} in AlpGen and Pythia.

Gen + Pythia 6 matched predictions, we have outlined a simple prescription to ensure this. This can be easily generalised, and applied to the case of matching AlpGen with other shower MCs, such as Herwig. We have then given an example of such a tune that compares well to Tevatron and LHC measurements of vector boson plus multijet final states. In addition, we have shown how consistent variations around a central ME-PS matched tune can be performed, so as to define a systematic uncertainty on that prediction. This knowledge should prove valuable in defining a new set of consistent ME-PS tunes for the precise future study of LHC multijet final states.

Acknowledgements

J. K. and L. M. acknowledge the support of the Initiative and Networking Fund of the Helmholtz Association, contract HA-101 (“Physics at the Terascale”). B. C. acknowledges the support of the UK Science and Technology Facilities Council (STFC). L. M. acknowledges the LPCC for the hospitality during the initial phase of this project.

A Appendix

A.1 An α_S Consistent AlpGen + Pythia 6 Tune

We here describe the parameters in the AlpGen and Pythia 6 codes that are important for ensuring the consistency of matching, and give the settings of these parameters which describe a new α_S consistent AlpGen + Pythia 6 tune. Note that the settings for Pythia are those of the central Perugia-2011 tune [6], which was inspired by these studies.

A.1.1 AlpGen Parameters

For AlpGen, the relevant parameters controlling the magnitude, renormalization scale, and running order for α_S are set to these values:⁶:

- The prefactor rescaling the value of the renormalization scale in the CKKW scale-setting procedure: `ktfac = 1.0`
- Λ_{QCD} (5-flavour): `xlc1u = 0.26`
- Running order: `lpc1u = 1`

A.1.2 Pythia Parameters

To the extent that the explanations given here are necessarily somewhat brief, we recommend the interested reader to follow up on the definitions of the parameters below in the program's comprehensive manual [2].

The Strong Coupling in Pythia 6: there are several different ways of specifying the parameters controlling α_S . In order for the user to have explicit control of all of them, we use the option `MSTP(3)=1`, which allows to specify formally independent Λ_{QCD} values for each of the different algorithmic components in Pythia. As a special case, we may then choose to set all those values equal, or at least set those equal that correspond to initial- and final-state radiation. These are:

- `PARP(61)` for Λ_{QCD} for ISR.
- `PARJ(81)` for Λ_{QCD} for FSR inside resonance decays.
- `PARP(72)` for Λ_{QCD} for FSR outside resonance decays (e.g., FSR off hard jets from the matrix element and/or from ISR).

The number of flavours with which to interpret Λ_{QCD} must also be specified. Since a value of $n_f = 5$ is hard-coded in at least one sub-algorithm of Pythia, we advise to always translate Λ_{QCD} values to 5-flavour ones and, correspondingly, set the n_f parameter `MSTU(112)=5`.

⁶The parameters `xlc1u` and `lpc1u` were introduced in connection with this work, and are implemented in AlpGen starting from v2.14. The default behaviour, if these parameters are not set, is to assign the values inherited from the PDF (as was the case for AlpGen versions before 2.14).

Further, in order to avoid that any of these values are modified by the code, we set $\text{MSTP}(64)=2$, and $\text{PARP}(64)=1.0$. The former forces the code to keep Λ_{QCD} unmodified for ISR. In particular, the translation from “MSbar” to “CMW”, which is applied for $\text{MSTP}(64)=3$, is *not* performed. This is equivalent to interpreting the effective Λ_{QCD} value as already being in a scheme similar to CMW. The latter, $\text{PARP}(64)=1.0$, sets the prefactor for the renormalization scale used for ISR equal to unity, i.e., the renormalization scale will just be p_T . Any re-interpretation of Λ_{QCD} , for instance to translate between different effective scheme definitions or to introduce multiplicative factors on the effective renormalization scale, for scale variation purposes, should then be imposed directly on the three Λ_{QCD} values above. This is the prescription followed in the so-called Perugia 2011 tunes which were developed as part of this effort, with parameters as listed in [6].

Finally, one needs to settle on an effective *value* for Λ_{QCD} . According to comprehensive Professor tunings [36, 37] of the p_T -ordered shower in Pythia [4] to event shapes and other LEP data, one needs values of order

$$\Lambda_{\text{QCD}}^{(5)} \sim 0.26, \quad (7)$$

where the superscript indicates the number of flavours. We interpret this as an effective value, derived directly from data using a “Pythia scheme” that is defined numerically by Pythia’s shower algorithm. It is not necessarily directly comparable to $\overline{\text{MS}}$ determinations⁷.

The Strong Coupling in Pythia 8: Although we restrict the numerical studies in this paper to Pythia 6, for completeness we also include the case of Pythia 8 [50], for which the corresponding relevant parameters are

- `TimeShower:alphaSvalue,`
- `TimeShower:alphaSorder,`
- `SpaceShower:alphaSvalue,`
- `SpaceShower:alphaSorder,`

for final-state (timelike) and initial-state (spacelike) showers, respectively. Notice in particular that one here specifies the value of $\alpha_s(M_Z)$ rather than that of Λ_{QCD} . Similar comments about the effective scheme definition as for Pythia 6 apply.

Radiation Phase Space: The size of the allowed phase space for radiation in the shower generator may also affect the matched result. In the p_T -ordered shower in Pythia 6, the switch $\text{MSTP}(72)$ controls the starting scale for final-state radiation off jets that are produced by initial-state radiation and/or are colour-connected to the beam. Naively, the FSR off such a parton should start at the scale at which it was created, which is obtained with $\text{MSTP}(72)=2$, the recommended option. Using the other available options is strongly discouraged, as these lead to a quite bad agreement with NLL resummations, underscored by Banfi et al in [51]. The Perugia 2011 tunes all use $\text{MSTP}(72)=2$.

⁷It is probably closest to the so-called CMW scheme [28]. For completeness, a reasonable derived guess for a corresponding $\overline{\text{MS}}$ value would then be ~ 0.16 , since the CMW prescription yields effective values that are approximately 1.6 times larger than the $\overline{\text{MS}}$ one.

Further, in the Perugia 2011 tunes, we start both the ISR and FSR evolutions at $p_{T\text{evol}} = \text{SCALUP}$, with the Pythia evolution variable $p_{T\text{evol}}$ defined in [4] and SCALUP the scale parameter defined in the Les Houches Accord for event generators [52, 53]. Technically, this is achieved by setting $\text{PARP}(71) = \text{PARP}(67) = 1.0$, where the former controls the scale factor applied to the starting scale for FSR and the latter sets the one for ISR. Note that these parameters could still be varied somewhat around their central values, since the $p_{T\text{evol}}$ variable used by Pythia is not 100% identical to the p_T definition that might be used to place cuts in a matrix-element generator, but we have not judged this difference essential at the current level of precision.

A.2 PYTHIA Tunes

In this work, we have used the Perugia 0, Perugia Hard, Perugia Soft, Perugia 2010, Perugia 2011, Perugia 2011 radHi, Perugia 2011 radLo [6], and the DW [7] tunes of Pythia 6.4 [2]. All use the CTEQ5L PDF set [33]. For a complete description, see the indicated references. The salient features of the tunes are as follows.

Tune DW [7] is a tune of the Q^2 -ordered shower. It is based on the Tevatron “Tune A”, which had great success in describing the underlying event measured at the Tevatron. Contrary to Tune A, however, DW also included the Drell-Yan p_T spectrum, for which Tune A predicted a far too soft spectrum. Tune DW therefore has a significantly lower renormalization scale for ISR (and thus a larger value of α_s), and 2 GeV of so-called “primordial k_\perp ”, as compared to 1 GeV in Tune A. The energy scaling of the underlying event was based on comparisons between the underlying-event level at the Tevatron between 630 and 1800 GeV.

The Perugia tunes [6] are all tunes of the p_T -ordered shower. Unlike DW, which was developed by tuning to the underlying event in jet events, the Perugia tunes primarily used minimum-bias data as drivers, relying on the universality of PYTHIA’s MPI modelling to extrapolate to the underlying event. In addition, a comprehensive update of the LEP fragmentation parameters was included in all tunes.

The first set, the Perugia 0 family, used LEP event shapes and fragmentation data, Tevatron minimum-bias data, and the Tevatron Drell-Yan p_T spectrum. Again, the scaling from Tevatron data at 630 GeV was used to determine the scaling with CM energy, with some additional constraints from older UA5 data also included. A “Hard” and “Soft” variation attempted to vary the shower radiation up and down, respectively. Both Perugia 0 and the “Hard” variation use the so-called “CMW” scheme for Λ_{QCD} for ISR, while the soft retained the unmodified $\overline{\text{MS}}$ value, in all cases taking the numerical value from the PDF set used. For the “Hard” variation, the renormalization scale for ISR was $0.5p_T$, for Perugia 0 p_T , and for the “Soft” variation, $\sqrt{2}p_T$. In addition, the “Hard” variation had higher-than-nominal values for FSR, and had a slightly harder hadronization spectrum, while the converse was true for the “Soft” one. None of these early tunes used the recommended $\text{MSTP}(72)=2$ setting, and hence predicted rather narrow ISR jets. The Pythia tune numbers are 320, 321, and 322, for Perugia 0, “Soft”, and “Hard”, respectively.

Tab.3 lists the parameter settings of the Perugia family that were used for the block variations in 2.2 .

In Perugia 2010, jet shapes were included among the tuning constraints. The amount of FSR outside resonance decays (previously controlled by the Λ_{QCD} value read from the PDF set) was adjusted to agree with the level inside them (constrained by fits to LEP event shapes), combined with the recommended $\text{MSTP}(72)=2$. The Λ_{QCD} value for ISR was still read from the PDF set, and translating from $\overline{\text{MS}}$ to CMW, as in Perugia 0. A few fragmentation parameters were slightly revised, since some of the previous ones had only been constrained using the Q^2 -ordered shower, and a new colour-reconnection model was introduced. No “Hard”

tuning block	parameter or switch	Perugia 0	Perugia hard	Perugia soft
ISR	PARP(64)	1.0	0.25	2.0
ISR	PARP(67)	1.0	4.0	0.25
ISR	MSTP(64)	3	3	2
FISR	PARP(71)	2.0	4.0	1.0
FISR	MSTP(72)	1	1	0
UE	PARP(82)	2.0	2.3	1.9
UE	PARP(83)	1.7	1.7	1.5
UE	PARP(90)	0.26	0.30	0.24
CR	PARP(77)	0.9	0.4	0.5
CR	PARP(78)	0.33	0.37	0.15

Table 3: Table of Perugia tune parameters relevant for this study. For a complete list see [6]

and “Soft” variations were produced for this tune. The Pythia tune number is 327 for Perugia 2010.

In Perugia 2011, it was possible to include some early lessons from LHC at 7 TeV. Based on observed strangeness and baryon production rates, a few of the fragmentation parameters were again revised. The universal effective Λ_{QCD} choice advocated in this paper was introduced. Variations labelled “radHi” and “radLo” were defined as well, expressing a factor 2 variation in the Λ_{QCD} values used for ISR and FSR. The Pythia tune numbers for Perugia 2011, radHi, and radLo, are 350, 351, and 352, respectively.

Tabulated values of the parameters of all of the Perugia tunes can be found in the appendices of [6].

References

- [1] C. Berger *et al.*, Phys.Rev.Lett. **106**, 092001 (2011), arXiv:1009.2338.
- [2] T. Sjöstrand, S. Mrenna, and P. Skands, JHEP **05**, 026 (2006), hep-ph/0603175.
- [3] M. L. Mangano, M. Moretti, F. Piccinini, R. Pittau, and A. D. Polosa, JHEP **07**, 001 (2003), hep-ph/0206293.
- [4] T. Sjöstrand and P. Z. Skands, Eur. Phys. J. **C39**, 129 (2005), arXiv:hep-ph/0408302.
- [5] P. Z. Skands, (2009), arXiv:0905.3418.
- [6] P. Z. Skands, Phys. Rev. **D82**, 074018 (2010), arXiv:1005.3457.
- [7] TeV4LHC QCD Working Group, M. G. Albrow *et al.*, (2006), arXiv:hep-ph/0610012.
- [8] T. Sjöstrand, Phys.Lett. **B157**, 321 (1985).
- [9] M. Bengtsson and T. Sjöstrand, Nucl.Phys. **B289**, 810 (1987).
- [10] G. Corcella *et al.*, JHEP **01**, 010 (2001), arXiv:hep-ph/0011363.
- [11] J. M. Butterworth, J. R. Forshaw, and M. H. Seymour, Z. Phys. C **72**, 637 (1996).
- [12] R. Corke and T. Sjöstrand, Eur.Phys.J. **C69**, 1 (2010), arXiv:1003.2384.
- [13] R. Corke and T. Sjöstrand, JHEP **1103**, 032 (2011), arXiv:1011.1759.
- [14] M. Bähr *et al.*, Eur. Phys. J. **C58**, 639 (2008), arXiv:0803.0883.
- [15] M. Cacciari and G. P. Salam, Phys. Lett. **B641**, 57 (2006), arXiv:hep-ph/0512210.
- [16] A. Buckley *et al.*, (2010), arXiv:1003.0694.
- [17] P. Skands *et al.*, in preparation, see <http://mcplots.cern.ch>.
- [18] M. L. Mangano, M. Moretti, F. Piccinini, and M. Treccani, JHEP **01**, 013 (2007), arXiv:hep-ph/0611129.
- [19] S. Mrenna and P. Richardson, JHEP **05**, 040 (2004), arXiv:hep-ph/0312274.
- [20] A. Buckley *et al.*, Physics Reports **504**, 145 (2011), arXiv:1101.2599.
- [21] P. Skands, (2011), arXiv:1104.2863, lectures presented at European School of High Energy Physics (ESHEP) June 2010, Raseborg, Finland.
- [22] S. Catani, F. Krauss, R. Kuhn, and B. R. Webber, JHEP **11**, 063 (2001), arXiv:hep-ph/0109231.
- [23] L. Lönnblad, JHEP **05**, 046 (2002), arXiv:hep-ph/0112284.
- [24] N. Lavesson and L. Lönnblad, JHEP **07**, 054 (2005), arXiv:hep-ph/0503293.
- [25] N. Lavesson and L. Lönnblad, JHEP **12**, 070 (2008), arXiv:0811.2912.

- [26] J. Alwall *et al.*, JHEP **0709**, 028 (2007), arXiv:0706.2334.
- [27] D. Amati, A. Bassetto, M. Ciafaloni, G. Marchesini, and G. Veneziano, Nucl. Phys. **B173**, 429 (1980).
- [28] S. Catani, B. R. Webber, and G. Marchesini, Nucl. Phys. **B349**, 635 (1991).
- [29] T. Gleisberg *et al.*, JHEP **0902**, 007 (2009), arXiv:0811.4622.
- [30] L. Lönnblad, Comput.Phys.Comm. **71**, 15 (1992).
- [31] P. Bartalini *et al.*, (2010), arXiv:1003.4220, 1st International Workshop, MPI'08, Perugia, Italy, October 2008.
- [32] CDF Collaboration, T. Aaltonen *et al.*, Phys. Rev. **D77**, 011108 (2008), arXiv:0711.4044.
- [33] CTEQ, H. L. Lai *et al.*, Eur. Phys. J. **C12**, 375 (2000), arXiv:hep-ph/9903282.
- [34] ATLAS Collaboration, CERN Report No. ATLAS-CONF-2011-060, 2011.
- [35] M. Cacciari and G. P. Salam, JHEP **0804**, 063 (2008), 0802.1189.
- [36] A. Buckley, H. Hoeth, H. Lacker, H. Schulz, and J. E. von Seggern, Eur. Phys. J. **C65**, 331 (2010), arXiv:0907.2973.
- [37] ATLAS Collaboration, (2011), ATL-PHYS-PUB-2011-008.
- [38] CDF Collaboration, CDF public note 10394, 2011.
- [39] CDF Collaboration, T. Aaltonen *et al.*, Phys. Rev. Lett. **100**, 102001 (2008), arXiv:0711.3717.
- [40] ATLAS Collaboration, G. Aad *et al.*, Phys.Lett.B (2010), arXiv:1012.5382.
- [41] D0 Collaboration, V. M. Abazov *et al.*, Phys. Lett. **B669**, 278 (2008), arXiv:0808.1296.
- [42] D0 Collaboration, V. M. Abazov *et al.*, Phys. Lett. **B678**, 45 (2009), arXiv:0903.1748.
- [43] D0 Collaboration, V. M. Abazov *et al.*, (2011), arXiv:1106.1457.
- [44] ATLAS Collaboration, CERN Report No. ATLAS-CONF-2011-042, 2011.
- [45] CMS Collaboration, CERN Report No. CMS-PAS-EWK-10-012, 2011.
- [46] CDF Collaboration, A. Abulencia *et al.*, Phys. Rev. **D74**, 071103 (2006), hep-ex/0512020.
- [47] CDF Collaboration, F. Abe *et al.*, Phys. Rev. **D45**, 1448 (1992).
- [48] ATLAS Collaboration, G. Aad *et al.*, Phys. Lett. **B698**, 325 (2011), arXiv:1101.0070.
- [49] CDF Collaboration, CDF note 8827 .
- [50] T. Sjöstrand, S. Mrenna, and P. Z. Skands, Comput. Phys. Commun. **178**, 852 (2008), arXiv:0710.3820.
- [51] A. Banfi, G. P. Salam, and G. Zanderighi, JHEP **1006**, 038 (2010), arXiv:1001.4082.
- [52] E. Boos *et al.*, (2001), arXiv:hep-ph/0109068.
- [53] J. Alwall *et al.*, Comput. Phys. Commun. **176**, 300 (2007), arXiv:hep-ph/0609017.